Pseudopotential total-energy study of the transition from rhombohedral graphite to diamond

S. Fahy, Steven G. Louie, and Marvin L. Cohen
Department of Physics, University of California, Berkeley, California 94720 and Materials and Molecular Research Division, Lawrence Berkeley Laboratory, University of California, Berkeley, California 94720
(Received 24 February 1986)

The path maintaining rhombohedral symmetry in the transition from graphite to diamond which minimizes the energy at each value of the bond length between layers is determined. The energy barrier for this path is found to be 0.33 eV. The total energy of the solid is calculated using local-density-functional theory with *ab initio* pseudopotentials. Results are presented for the charge density and density of states along the transition path. In contrast to recent extended-Hückel-theory results, throughout most of the transition the structure is found to remain semimetallic or semiconducting. A final rapid opening of the gap to the insulating diamond phase develops as the interlayer carbon-carbon bonds form. The behavior of rhombohedral graphite under conditions of isotropic pressure is also examined. We predict that rhombohedral graphite will transform to diamond, without thermal or catalytic activation, at an isotropic pressure of 80 GPa if it maintains its rhombohedral symmetry. Our analysis moreover suggests that, in general, cross linking of hexagonal-ring carbon compounds leading to local tetrahedral coordination should be favored when the interlayer distance between hexagonal rings is between 2.1 and 2.3 Å.

I. INTRODUCTION

Natural graphite occurs in two crystal structures: the more common, hexagonal or Bernal structure,[1] and the rhombohedral structure.[2] A given sample usually contains 5–15% of the rhombohedral structure intermixed in a mosaic combination with the hexagonal form and with disordered graphite.[2,3] Crystals of almost pure hexagonal graphite can be made by heat treatment and quenching, but the rhomobohedral form has not been obtained in isolation from the hexagonal structure.

Both forms of graphite consist of planes of carbon atoms each forming a hexagonal net with a nearest-neighbor distance of 1.42 Å, stacked with an interplanar spacing of 3.35 Å (Fig. 1). They differ, however, in the stacking sequence of the planes. The hexagonal structure has an *AB* stacking, with half of the atoms directly above each other in adjacent planes and the other half directly above the center of the hexagonal ring in the adjacent plane. The rhombohedral structure has an ABC stacking; half of the atoms are directly below atoms in the adjacent plane and directly above hexagonal ring centers, and the other half of the atoms are directly above atoms and below hexagonal ring centers. The rhombohedral structure can be obtained from the hexagonal structure by slipping every third plane, as shown in Fig. 1.

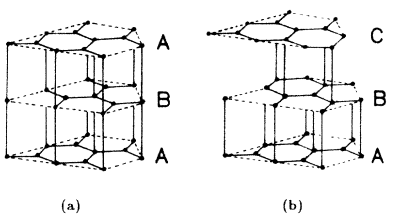

FIG. 1. The crystal structure of (a) hexagonal and (b) rhombohedral graphite showing the different stacking of the layers.

In this paper we will concentrate exclusively on the rhombohedral graphite structure because of the following simple geometrical relationship[4] between it and the diamond structure (Fig. 2): Although the diamond structure has additional symmetries, both are cases of the more general rhombohedral structure characterized by the bond length between layers, R, the bond length within layers, B, and the buckling angle, θ, between them.[5] The diamond structure is obtained when $R=B=1.54$ Å and θ is the ideal tetrahedral angle, 109.47°. In this case the rhombohedral bravais lattice becomes the face-centered-cubic lattice, and the vertical direction is the [111] direction of the usual cubic description of the diamond structure. The rhombohedral graphite structure is obtained when $\theta=90°$, $R=3.35$ Å, and $B=1.42$ Å. In this scheme, the diamond structure is viewed as a set of buckled planes stacked in *ABC* sequence in the [111] direction. We can continuous-

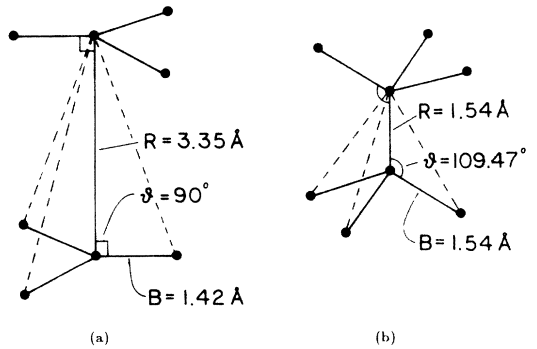

FIG. 2. The local structure of (a) rhombohedral graphite (b) diamond. The dashed lines indicate the basis vectors of the rhombohedral lattice. The [111] direction of the usual cubic description of the diamond lattice is vertical.

ly transform rhombohedral graphite into diamond by reducing the bond length between layers while simultaneously increasing the buckling angle and the bond length within layers. Throughout the transformation, the rhombohedral symmetry can be maintained; all the intervening structures having a rhombohedral bravais lattice and space group, D_{3d}^5.

This transformation has recently been studied by Kertesz and Hoffmann[6] using extended-Hückel band calculations to find the path which minimizes the energy of the solid at each value of the interlayer bond length. The present work uses the density-functional formalism[7,8] and *ab initio* pseudopotentials[9] with a localized orbital basis[10] to study the transformation from first principles. This method has been used in the past to obtain very accurate structural properties for carbon in the solid-state environment.[11] A more reliable profile of the total energy of the structure and of the variation of the structural parameters, R, B, and θ, is thereby obtained. We also determine the charge density and density of states for the crystal as the transformation proceeds.

The path which minimizes the total energy of the solid at each value of the interlayer bond length in the transformation is found to have an energy barrier of 0.33 eV per atom; the energies of the initial graphite and final diamond structures are very nearly equal. As the graphite interlayer bond distance is decreased, the increase in the buckling angle and the intralayer bond length is very slow initially; only when the interlayer bond is 2.3 Å does the intralayer bond length begin to increase significantly. At this point the buckling angle θ is 97°. Analysis of the charge density reveals that the characteristic double peak in the density along the carbon-carbon bond does not develop in the bond between layers until its length is within 10—15% of its value in the diamond structure. The density of states for the intermediate structures show that the crystal remains semiconducting or semimetallic for most of this path. Only when the double peak of the carbon-carbon bond between layers forms does a significant gap open between the valence and conduction bands causing the structure to become insulating. In contrast to the results of Ref. 6, a large density of states at the Fermi level is not found for structures on the transition path.

We have also determined the behavior of rhombohedral graphite under hydrostatic pressure. Assuming rhombohedral symmetry is maintained, the graphite structure is found to remain metastable up to a maximum of 80 GPa. At pressures above 80 GPa, only the diamond form (i.e., the special case of the rhombohedral structure for which $R=B$ and $\theta=109.47°$) is stable or metastable. Thus, as the pressure is increased from 0 to 80 GPa, the structural parameters vary continuously from $R=3.35$ Å, $B=1.42$ Å, $\theta=90°$, to $R=2.1$ Å, $B=1.38$ Å, $\theta=97°$. As the pressure is further increased above 80 GPa, it is no longer possible to maintain metastability (i.e., to find a local minimum of the free energy, $E+PV$) by continuously varying the structural parameters, and the only local minimum of the free energy occurs for the diamond structure. This maximum pressure of 80 GPa is an *upper* bound for the metastability of rhombohedral graphite since instabilities which do not maintain rhombohedral symmetry may occur at lower pressures.

A careful examination of the band structure near the conduction-band minimum and valence-band maximum for rhombohedral graphite at zero pressure shows that, unlike hexagonal graphite, it is not a semimetal but rather a semiconductor with a small direct gap of approximately 0.05 eV. This calculated gap is probably an underestimate since a local-density formalism is used. This finding shows that the existence of a Fermi surface is sensitive to the stacking of the layers, a point of general significance for pure (i.e., undoped) graphite. It is experimentally observed that in the pyrolitic form, where the layers are well formed but their stacking is poorly characterized, graphite behaves as a semiconductor.[12]

The remaining four sections of the paper are as follows: In Sec. II we will describe in detail the calculation of the total energy of the solid and the results obtained. In Sec. III the results of the charge density and density of states calculations are presented. In Sec. IV we consider the nature of the bonding in the solid in three different phases of the transformation from graphite to diamond in the light of the results presented for the total energy, charge density, and density of states. We also discuss the absence of a Fermi surface in rhombohedral graphite as well as the absence of metallic structures which were predicted[6] to exist on the continuous transition path from rhombohedral graphite to diamond. Finally, in Sec. V, we present the main conclusions of this study.

II. TOTAL ENERGY

The total energy per cell (two atoms) of the general rhombohedral structure is a function $E(R,B,\theta)$; that is, a function of the three parameters used to specify it (R equals the bond length between layers, B equals the bond length within layers, and θ is the buckling angle). Following the convention of Kertesz and Hoffmann,[6] we can treat R as the independent variable in transforming rhombohedral graphite into diamond. The parameters B and θ are then varied for each given value of R to minimize the total energy, $E(R,B,\theta)$, while maintaining rhombohedral symmetry. Thus we obtain three functions of R (Fig. 3): $E_{\min}(R)$ is the minimum value of $E(R,B,\theta)$ for a given value of R; $B_{\min}(R)$ is the value of B at which this minimum occurs; $\theta_{\min}(R)$ is the value of θ at which the minimum occurs.

To determine the effect of hydrostatic pressure on rhombohedral graphite, we treat the cell volume V as the independent variable and vary B and θ to find a local minimum of the total energy for each given value of V. Thus we obtain the functions, $E_{\min}(V)$, $B_{\min}(V)$, and $\theta_{\min}(V)$, as shown in Fig. 4. These functions are defined in the same way as the analogous functions for R. Two branches (i.e. two local minima) exist for cell volumes greater than 11.0 Å^3. One is the diamond structure, for which $R=B$ and $\theta=109.47°$; the other is a compressed form of graphite with R between 2.1 and 3.35 Å, B between 1.37 and 1.42 Å, and θ between 90° and 97°. For cell volumes less than 11.0 Å^3, only the diamond branch exists. The pressure on either branch is given by $-dE_{\min}(V)/dV$.

The total energy is calculated within local-density-functional theory[7,8] using the formalism of Ihm *et al*[13] The electron-ion interaction is determined using *ab initio* pseudopotentials generated by the scheme of Hamann, Schluter, and Chiang[9] and the exchange-correlation energy is evaluated with the function of Hedin and Lundqvist.[14] We express the total energy as a sum of terms:

$$E_{\text{tot}}=E_{c\text{-}c}+E_{\text{kin}}+E_{e\text{-}c}+E_{e\text{-}e} \ , \tag{1}$$

where $E_{c\text{-}c}$ is the core-core Coulomb interaction (Ewald term), E_{kin} is the kinetic energy of the electrons, $E_{e\text{-}c}$ is the electron-core interaction (determined using the ion pseudopotential), and $E_{e\text{-}e}$ is the electron-electron interaction (Hartree and exchange-correlation terms).

We determine $E_{\text{kin}}+E_{e\text{-}c}+E_{e\text{-}e}$ as follows: The Kohn-Sham equations,[8]

$$\left[-\frac{\hbar^2\nabla^2}{2m}+V_{\text{ion}}(\mathbf{r})+V_H(\mathbf{r})+\mu_{\text{xc}}(\mathbf{r})\right]\psi_i(\mathbf{r})=\varepsilon_i\psi_i(\mathbf{r}) \ , \tag{2}$$

are solved self-consistently. Here, V_{ion} is the sum of the ion pseudopotentials; V_H is the Hartree potential due to

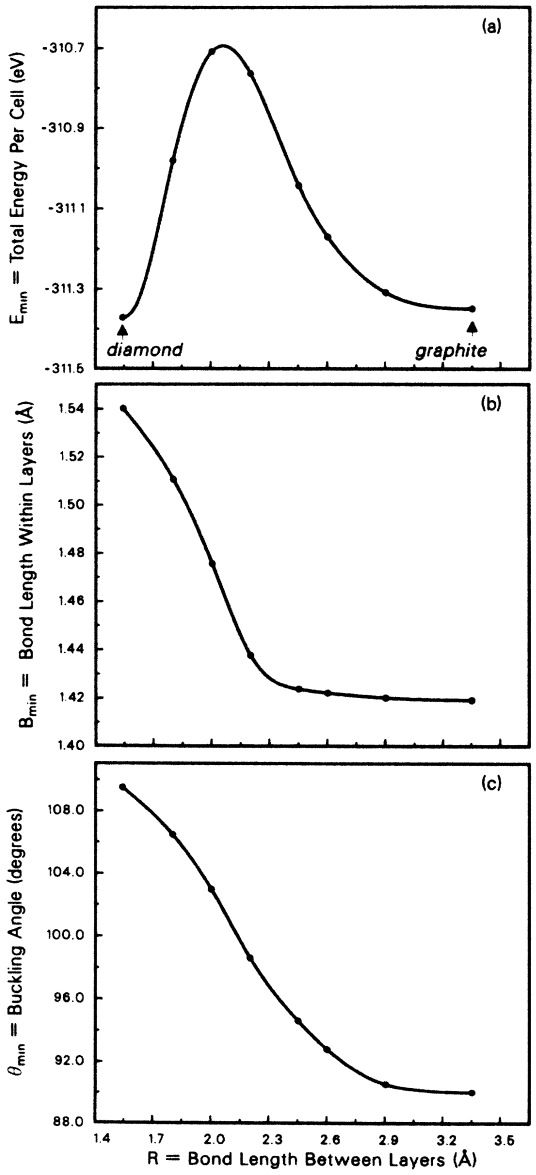

FIG. 3. (a) Total energy per cell (two atoms), (b) bond length within layers, and (c) buckling angle as functions of the bond length between layers for the path which minimizes the total energy for each value of the interlayer bond length. The points are calculated and the curves are cubic spline interpolations between them.

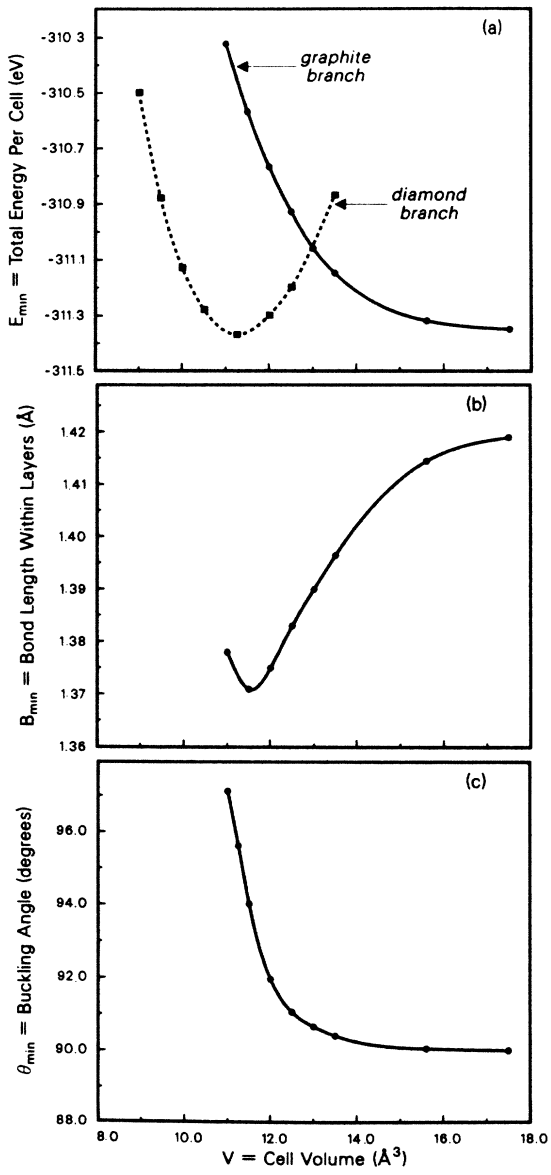

FIG. 4. (a) Total energy per cell (two atoms), (b) bond length within layers, and (c) buckling angle as functions of the cell volume for the hydrostatic pressure path. In (a) the solid curve is for the graphite branch and the dashed curve is for the diamond branch. The diamond branch is not shown in (b) or (c). The points are calculated and the curves are cubic spline interpolations between them.

the valence charge density,

$$\rho(\mathbf{r})=e\sum_{\varepsilon_i<E_F}|\psi_i(\mathbf{r})|^2, \tag{3}$$

where E_F is the Fermi level; and $\mu_{xc}(\mathbf{r})$ is the exchange-correlation potential for the charge density $\rho(\mathbf{r})$. The sum of the electron kinetic, electron-core, and electron-electron energies is given by

$$E_{\text{kin}}+E_{e\text{-}c}+E_{e\text{-}e}=\sum_{\varepsilon_i<E_F}\varepsilon_i-\tfrac{1}{2}\int V_H(\mathbf{r})\rho(\mathbf{r})d\mathbf{r}-\int\mu_{ex}(\mathbf{r})\rho(\mathbf{r})d\mathbf{r}+\int\varepsilon_{xc}(\mathbf{r})\rho(\mathbf{r})d\mathbf{r}, \tag{4}$$

where $\varepsilon_{xc}(\mathbf{r})\rho(\mathbf{r})$ is the exchange-correlation energy density. Equation (4) correctly accounts for overcounting of the Coulomb interaction between the electrons in the sum of eigenvalues, unlike the extended-Hückel technique where the total energy is expressed simply as a sum of eigenvalues. Variations in the core-core interaction energy as a function of the structural parameters are also neglected in the extended-Hückel calculations.

The wave functions are expanded in a linear combination of localized orbitals with s and p symmetry centered on the atomic sites[10] of the form

$$f_{\alpha lm}(\mathbf{r})=A_{\alpha lm}e^{-\alpha r^2}r^l K_{lm}(\theta,\phi), \tag{5}$$

where $A_{\alpha lm}$ are normalization constants, and K_{lm} are "Kubic harmonics". Sixteen orbitals per atom are used and the values of the radial Gaussian decays, α, are chosen for each structure to minimize the total energy.[15] The potential is made fully self-consistent using the scheme of Chan *et al.*[16] with plane-wave components up to an energy of 64 Ry. A uniform grid of 19 **k** points in the irreducible sector of the Brillouin zone is used.[17]

The quantities $E_{\min}(R)$, $B_{\min}(R)$, and $\theta_{\min}(R)$ were all determined for eight values of R (i.e., for the ideal graphite and diamond values of R and for six intermediate values). For the values of R corresponding to the ideal graphite and diamond structures, the values of $B_{\min}(R)$ and $\theta_{\min}(R)$ are within 0.1% of the experimentally measured values. We have overestimated the binding of diamond with respect to graphite by 0.009 eV per atom as compared with experiment[18] but this is within the uncertainty in the energy due to numerical approximations in the method. We estimate all the values of $B_{\min}(R)$ and $\theta_{\min}(R)$ evaluated in this calculation are reliable within 0.1% and the relative energies of the structures are correct to within 0.01 eV per atom.

The energy barrier for this transition path is 0.33 eV per atom [see Fig. 3(a)]. The maximum energy along the path occurs at the point $R=2.07$ Å, $B=1.48$ Å, and $\theta=101.4°$, which is a saddle point of the energy $E(R,B,\theta)$. Assuming that this is the only saddle point, as is likely to be the case, it follows that any continuous path from rhombohedral graphite to diamond which maintains rhombohedral symmetry must have an energy barrier of at least 0.33 eV per atom. Of course, if the restriction of rhombohedral symmetry is not imposed, it may be possible to find a path with a lower energy barrier.

The hydrostatic pressure path does not lead continuously from graphite to diamond. The graphite branch terminates when the cell volume equals 11.0 Å^3, at which point $R=2.1$ Å, $B=1.38$ Å, and $\theta=97°$, and the pressure equals 80 GPa. As can be seen from Fig. 4(a), this path does not pass through any saddle points of the total energy. At the termination point of the graphite branch, the stationary point of the total energy function restricted to the surface of constant volume becomes an inflection point, whereas for greater volumes it is a local minimum.

III. CHARGE DENSITY AND DENSITY OF STATES

The charge density and electronic density of states (Figs. 5 and 6) were evaluated for various structures along the calculated path shown in Fig. 3, which minimizes the energy at each value of R. For this calculation, a uniform grid of 85 **k** points in the irreducible Brillouin zone (equivalent to 729 points in the full Brillouin zone) was used. The Fourier components of the ground-state charge density are found as part of the total-energy calculation[16] and from these the real-space charge densities in Fig. 5 are calculated. The density of states is calculated from the eigenvalues on the 85 **k**-point grid using a tetrahedral integration scheme.[19] The use of 85 **k** points is sufficient to obtain a reasonably good density of states. There is undoubtedly some noise in the results presented in Fig. 6, hence fine details may not be reproduced exactly. However, all the main features of the band structures of diamond[10] and graphite[20] are expected to be reliable. In this study, we are concerned with the main features of the electronic structure. In particular, whether a structure is insulating, semiconducting, semimetallic or metallic depends on the density of states in the region of the Fermi level. With only 85 **k** points it is not possible to distinguish reliably between a semimetal with a small overlap between the conduction and valence bands and a semiconductor with a small gap (at the level of 0.1 eV); but the distinction between these two and either an insulator or a metal is unambiguous. In general, local-density-functional theory gives band gaps which are 20—50% too small compared with experiment for insulators and semiconductors.[21] However, the qualitative nature of the spectrum (i.e., whether a gap exists or not) is in general predicted correctly. Furthermore, the pressure dependencies of the gaps in many materials, including diamond, is prediced correctly by local-density-functional theory.[22]

From the results presented in Fig. 6, we see that as R is reduced from 3.35 to 1.8 Å the structure is always either

semiconducting or semimetallic. As R is finally reduced to its value for the diamond structure, the gap (initially direct at Γ for $R=1.8$ Å but becoming indirect as the diamond structure forms) opens to a value of 4.3 eV.[23] Analysis of the individual eigenvalues shows that, except for diamond, in each structure ($R=1.8$, 1.88, 2.07, 2.5, 3.35 Å) for which the density of states is calculated, the maximum of the valence band is in the same region of the Brillouin zone as the minimum of the conduction band. For ideal rhombohedral graphite, this region lay close to the Brillouin zone boundary as it does in hexagonal graphite. As the interlayer distance is reduced, it moves into the interior of the zone and finally converges on the center of the zone for $R=1.8$ Å.

Because of the interest[3,24] in whether ideal rhombohedral graphite is a semiconductor or a semimetal, we calculated the band structure on a very fine mesh in the region of the valence-band maximum and conduction-band minimum for this structure. We find that within the local-density approximation the structure is a semiconductor with a small direct gap of approximately 0.05 eV. The gap is located very close to the region where earlier two-band models[3,24] had predicted touching of the bands.

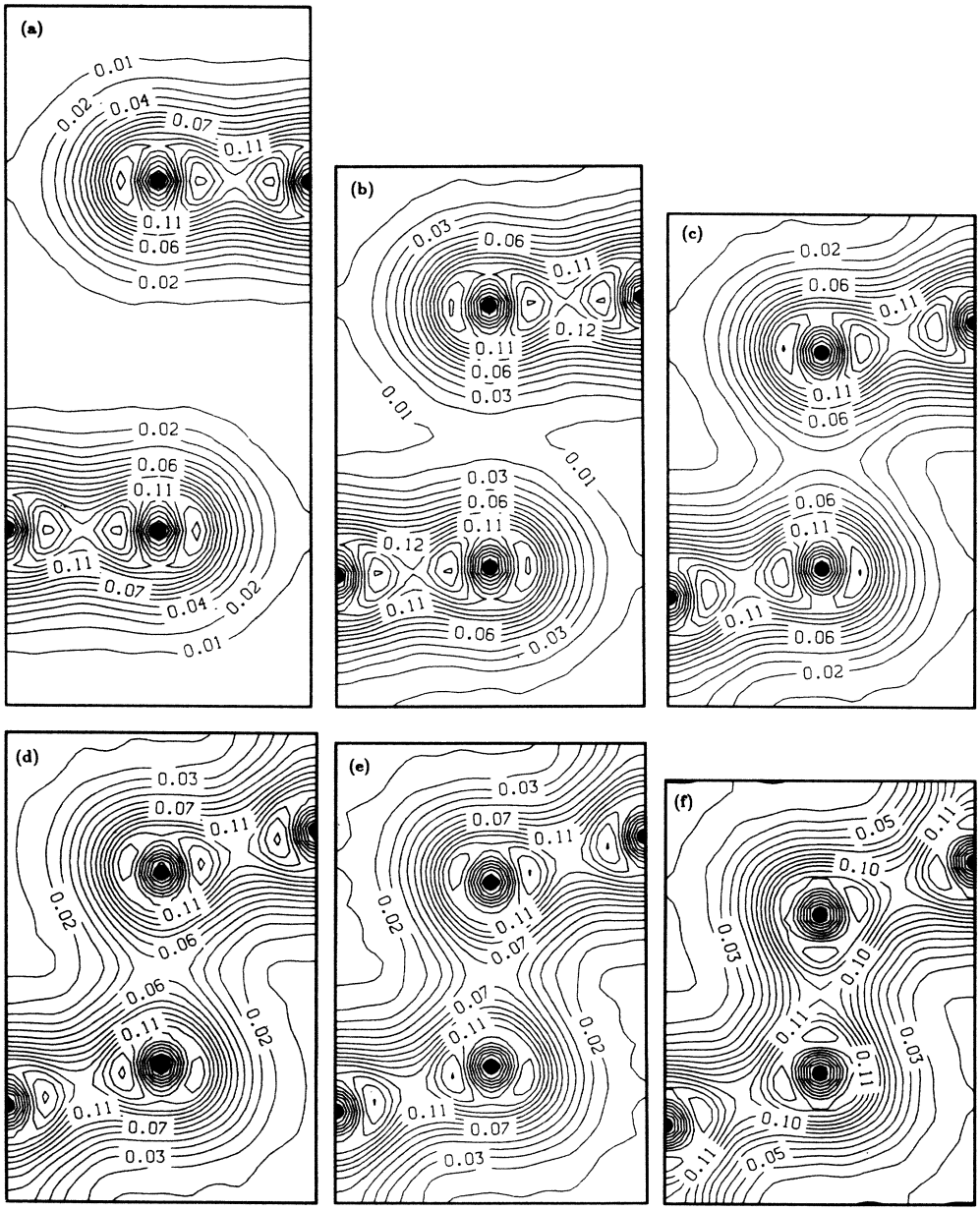

FIG. 5. Charge density in the plane containing a bond located between layers and a bond lying within layers, for various points on the path which minimizes the energy for each value of the interlayer bond length, R. The filled circles indicate the atomic positions. The values of R are (a) 3.35 Å, (b) 2.5 Å, (c) 2.07 Å, (d) 1.88 Å, (e) 1.8 Å, (f) 1.54 Å.

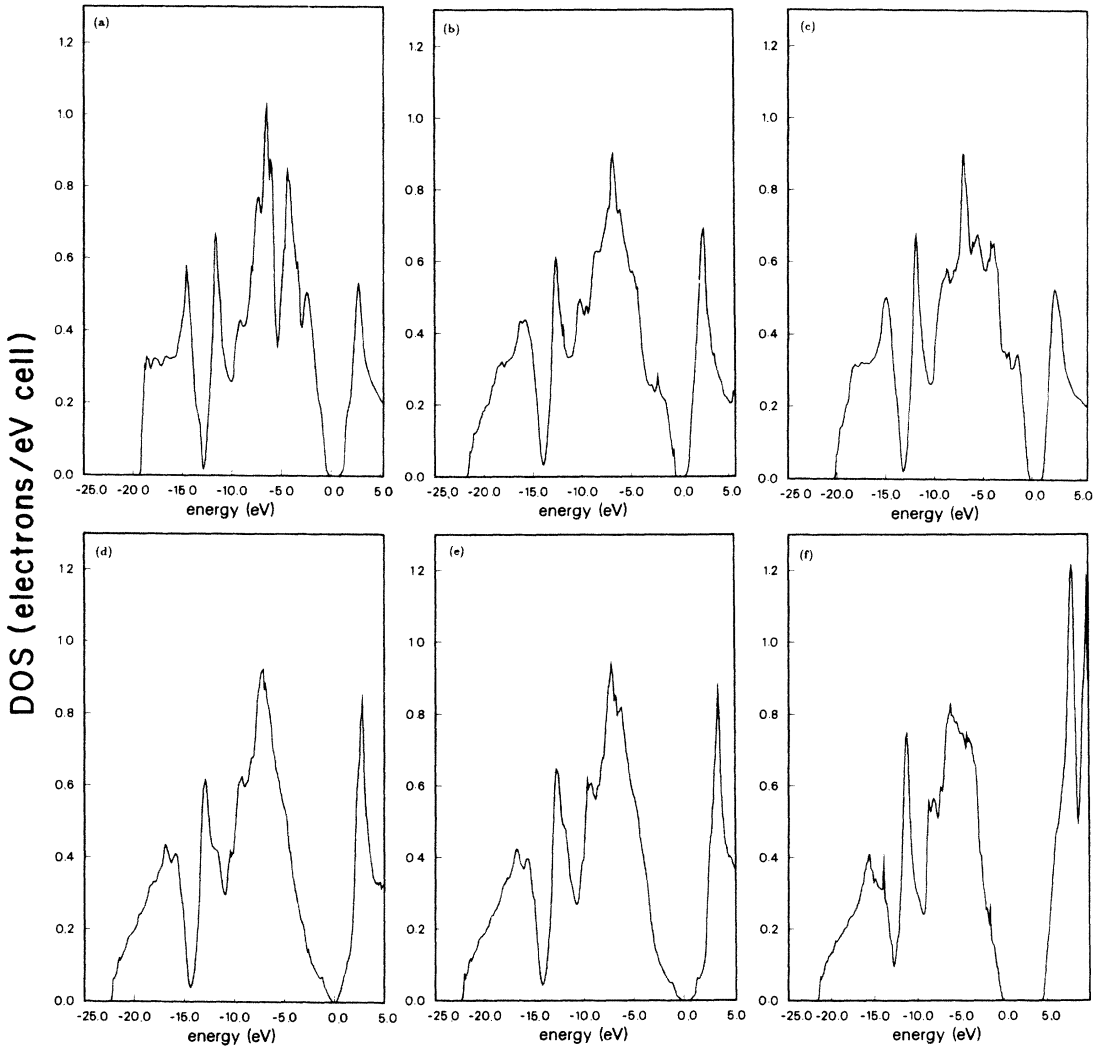

FIG. 6. Density of states (in units of electrons/eV cell) for various points on the path which minimizes the energy for each value of the interlayer bond length. The lettering refers to the same structures as in Fig. 5. The zero of energy is at the Fermi level in each case.

IV. DISCUSSION

If rhombohedral graphite maintains its rhombohedral symmetry under hydrostatic pressure, then the results presented here predict that the structure should transform to diamond when the pressure is approximately 80 GPa. This transformation is expected to occur without thermal or catalytic activation. However, there are other, more complex possiblities for the behavior of rhombohedral graphite under pressure (e.g., spontaneous shearing parallel to the layers resulting in a different stacking sequence, or complex cross-linking in the manner discussed in Ref. 12).

When the interlayer bond length is the constrained variable, we find that as the interlayer bond length in graphite is reduced from its initial value of 3.35 Å [Fig. 5(a)] to 2.5 Å [Fig. 5(b)], the charge density in the region between the layers remains very small and almost homogeneous. When the interlayer bond length is further reduced to 2.07 Å [Fig. 5(c)], significant inhomogeneity in the charge density between the layers has already developed, with a clearly defined accumulation of charge along the line of the interlayer bond. We also observe that the peak in the charge density along the intralayer bond has decreased noticeably. This trend continues as the intralayer bond length increases further to its value in the diamond structure. A peak in the charge density along the interlayer bond does not arise until the length of the bond is less than 1.8 Å [it is not present in Fig. 5(e)]. Only as this peak develops does a significant gap arise in the density of states between the valence and conduction bands [see Figs. 6(e) and 6(f)].

The behavior of the exchange-correlation energy,

$$E_{xc} = \int \varepsilon_{xc}(\mathbf{r})\rho(\mathbf{r})d\mathbf{r} \tag{6}$$

with changing R illustrates the different nature of the bonding in three phases of the transformation (Fig. 7). As the distance between the layers is decreased from its value in ideal graphite and the charge density between the layers

increases, E_{xc} becomes more negative initially ($dE_{xc}/dR > 0$). Then, as the intralayer bond length starts to increase significantly and the peak in the charge density along it starts to decrease, dE_{xc}/dR changes sign and E_{xc} becomes rapidly less negative. Finally, as the structure becomes insulating and strong bonds form between the layers, dE_{xc}/dR changes sign again and E_{xc} becomes rapidly more negative. Of course the exchange-correlation energy is only one term in the total energy of the solid and should not be considered to determine the preferred bonding configuration on its own. For instance, in the first of the three phases of the transformation discussed here, although the exchange-correlation energy is decreasing, the total energy is increasing. The results presented in Fig. 7 merely reflect the fact that the exchange-correlation energy favors the inhomogeneous charge distribution associated with the formation of localized bonds.[25]

Even with its restriction of rhombohedral symmetry, the analysis presented here of graphite under hydrostatic pressure or under constraint of the bond length between layers provides insight into the breakdown of carbon sp^2 bonding and the formation of tetrahedral bonds in general. When the interlayer bond length is constrained (see Fig. 3), the maximum of $-dE_{min}(R)/dR$ occurs at the same point ($R=2.3$ Å) as the start of elongation of the bonds within layers. It is also at this point that significant inhomogeneity in the charge density between layers begins to develop. Clearly the integrity of the graphite layers begins to be lost at this point, which indicates that the sp^2 classification of the bonding in the solid which is appropriate for graphite[26] begins to break down here. On the other hand, sp^3 classification which is good for diamond does not seem appropriate until the interlayer bond length is less than 1.8 Å. However, the formation of tetrahedral bonds clearly becomes more favorable than the formation of sp^2 bonds once R is less than 2.1 Å.

Although constraint of the interlayer bond length is a very different condition from the imposition of hydrostatic pressure, in the latter case the breakdown of sp^2 bonding also seems to occur when the interlayer bond length is approximately 2.3 Å. It is clear from Figs. 4(b) and 4(c) that the graphite layers start to change drastically in the region between $V=12.0$ Å^3 and $V=11.5$ Å^3. In this region, the interlayer bond length has values between 2.3 and 2.4 Å. Furthermore, the fact that the graphitic branch of the hydrostatic pressure curve becomes unstable at $V=11.0$ Å^3, when $R=2.1$ Å, is again consistent with the idea that the tendency to form tetrahedral bonds dominates when the interlayer bond length is less than 2.1 Å. These facts all suggest that local bonding properties govern the course of the transformation in the highly compressed regime and that, in general, cross linking of hexagonal-ring carbon compounds leading to local tetrahedral coordination should be favored when the distance between hexagonal rings is between 2.1 Å and 2.3 Å.[12]

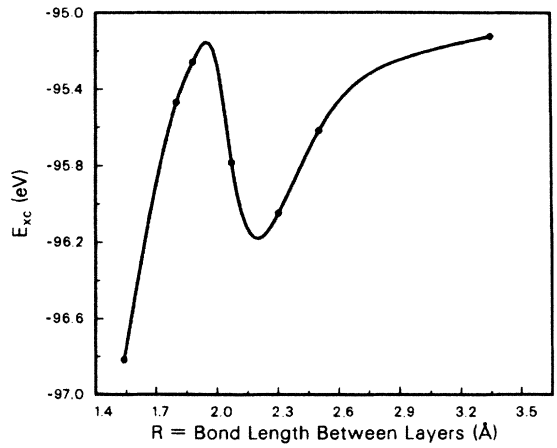

FIG. 7. The exchange-correlation energy per cell as a function of the bond length between layers for the path which minimizes the energy for each value of the interlayer bond length. The points are calculated and the curve is a cubic spline interpolation between them.

Contrary to the results of Kertesz and Hoffmann,[6] we do not find metallic behavior for any of the structures along the transition path, which minimizes the total energy at each value of the interlayer bond length from rhombohedral graphite to diamond. As pointed out by these authors, the symmetry of the wave functions at the Γ point for graphite and for diamond forces an accidental degeneracy of the conduction and valence bands at Γ for some structure along the transition path. We observe this degeneracy in our calculation when R is approximately 1.85 Å. In general, the maximum of the valence and the minimum of the conduction bands need not occur at or near Γ, so that degeneracy of the bands at this point would force metallic filling of the bands. However, we observe that in the present calculation, the maximum of the valence and the minimum of the conduction bands do indeed occur at or near Γ when the bands are degenerate at Γ. This is why there is no significant density of states at the Fermi level for the structures examined.

The two-band tight-binding calculations of Haering[3] and McClure[24] indicated the presence of a Fermi surface in rhombohedral graphite in approximately the same regions of reciprocal space where the Fermi surface of hexagonal graphite lies. In the hexagonal structure the crystal symmetry forces a degeneracy of the valence and conduction bands at points on the six vertical edges of the Brillouin zone; dispersion of the bands along these edges then gives rise to the Fermi surface. No such symmetry in the rhombohedral structure forces the existence of a Fermi surface and the accidental degeneracy which causes one to occur in the two-band model is lifted in a calculation which allows for hybridization between the p_z orbitals (which are the main components of the π bands) and the s, p_x and p_y orbitals. We see then that modifications of the stacking sequence in graphite may alter or destroy the Fermi surface and in turn significantly affect the electrical conductivity. It has been observed[12] that single-crystal hexagonal graphite has a conductivity 2—10 times that of pyrolitic graphite at room temperature. This effect could be explained either by alteration or destruction of the Fermi surface leading to a lower carrier concentration in the pyrolitic form or by a shorter mean free path due to a higher concentration of scattering defects in the

crystal. However, the fact that the temperature variation of the conductivity is semiconductorlike in pyrolitic graphite while it is semimetal-like in the pure hexagonal form is explicable only in terms of band structure effects.

V. CONCLUSION

We have presented an analysis, from first principles, of a continuous transition path from rhombohedral graphite to diamond. The path maintaining rhombohedral symmetry which minimizes the total energy of the solid for each value of the interlayer bond length is determined. The graphite layers are found to maintain their essential integrity, with little change in bond length within the layers, until the interlayer bond length is reduced to 2.3 Å. After that point the bond length within the layers increases rapidly to its value in the diamond structure as the bond between layers shortens. The energy barrier for this path is 0.33 eV per atom.

The charge density shows that as the interlayer bond length is reduced, although charge begins to build up in the bond between layers at about the same time as the bond length within layers begins to increase substantially, it is not until the length of the interlayer bond is within 10—15 % of its value in the diamond structure that the characteristic double peak of the carbon-carbon bond develops there. The density of electronic states reveals that the structure is semimetallic or semiconducting during most of the transition from graphite to diamond. Only as the double peak of the charge density in the bond between layers develops does the gap open to that of the insulating diamond structure. The rhombohedral graphite structure is found to be semiconducting with a small direct gap of 0.05 eV.

The behavior of rhombohedral graphite under hydrostatic pressure is also determined. Assuming rhombohedral symmetry is maintained, a graphiticlike structure is found to be metastable up to approximately 80 GPa, at which point the density is 60% greater than graphite at zero pressure and 2% greater than diamond at zero pressure. Above 80 GPa we find that the only stable or metastable structure with the rhombohedral symmetry assumed here is the diamond structure. Our results suggest that, in general, cross linking of hexagonal ring carbon compounds leading to local tetrahedral coordination should be favored when the interlayer distance between hexagonal rings is between 2.1 and 2.3 Å.

ACKNOWLEDGMENTS

We thank C. T. Chan for many helpful suggestions and discussions. Discussions with D. Tomanek, S. H. Liu, and S. L. Richardson concerning chemical notation are acknowledged. This work was supported by National Science Foundation Grant No. DMR-831-19024 and by the Director, Office of Energy Research, Office of Basic Sciences, Materials Sciences Division of the U.S. Department of Energy under Contract No. DE-AC03-76SF00098. A NSF supercomputer time grant at Purdue University Computing Center is also acknowledged. S. F. wishes to thank the National University of Ireland for financial support.

[1]J. D. Bernal, Proc. R. Soc. London, Ser. A **160**, 749 (1924).

[2]H. Lipson and A. R. Stokes, Proc. R. Soc. London, Ser. A **181**, 101 (1942).

[3]R. R. Haering, Can. J. Phys. **36**, 352 (1958).

[4]It appears that this relationship between diamond and graphite was first pointed out by N. Nath, Proc. Indian Acad. Sci. **2**, 143 (1935).

[5]The bond line between layers (i.e., the vertical bond line in Fig. 2) is a threefold rotation axis and the center of the bond is an inversion center in the general structure. The structure also has mirror symmetry in the plane formed by the bond line between layers and any one of the three bond lines within the layer.

[6]M. Kertesz and R. Hoffmann, J. Solid State Chem. **54**, 313 (1984).

[7]P. Hohenberg and W. Kohn, Phys. Rev. **136**, B864 (1964).

[8]W. Kohn and L. J. Sham, Phys. Rev. **140** A1133 (1965).

[9]D. R. Hamann, M. Schluter, and C. Chiang, Phys. Rev. Lett. **43**, 1494 (1979).

[10]J. R. Chelikowsky and S. G. Louie, Phys. Rev. B **29**, 3470 (1984).

[11]D. Vanderbilt and S. G. Louie, Phys. Rev. B **29**, 7099 (1984); D. Vanderbilt and S. G. Louie, Phys. Rev. B **30**, 6118 (1984); D. Vanderbilt, S. G. Louie, and M. L. Cohen, Phys. Rev. Lett. **53**, 1477 (1984); M. Hanfland, K. Syassen, S. Fahy, S. G. Louie, and M. L. Cohen, Phys. Rev. B **31**, 6896 (1985).

[12]H. G. Drickamer, in *Solid State Physics,* edited by H. Ehrenreich, F. Seitz, and D. Turnbull (Academic, New York, 1965), Vol. 17.

[13]J. Ihm, A. Zunger, and M. L. Cohen, J. Phys. C **12**, 4409 (1979).

[14]L. Hedin and B. I. Lundqvist, J. Phys. C **4**, 2064 (1971).

[15]Four radial decays per atom were used, with four orbitals, s,p_x,p_y,p_z for each decay. A full minimization of the energy with respect to all four decays for each structure individually would be prohibitively expensive (over 160 structures were considered in all) and in fact proves unnecessary. The following procedure was used in this calculation: The values of the decays were chosen to be in geometric progression so that once the smallest and largest decays are chosen, the other two are determined. A full minimization with respect to the geometric-progression decays was performed for diamond and also for ideal rhombohedral graphite. These two sets of decays proved to be very similar; the largest decay for diamond was 2.9 in atomic units and the smallest 0.23, while for graphite the largest was 2.95 and the smallest 0.19. For the intermediate structures between graphite and diamond, the geometric-progression decays were determined by linear interpolation of the largest and smallest decays with respect to the parameter RB^2 between the graphite and the diamond structures. We estimate the error in the relative total energies per cell from these approximations to be less than 0.01 eV.

[16]C. T. Chan, D. Vanderbilt, and S. G. Louie, Phys. Rev. B **33**, 2455 (1986), **34**, 8791(E) (1986).

[17]The calculation was also performed for a number of structures with 32 and 85 **k** points to check convergence. The total en-

ergy per cell in all cases changed by less than 0.02 eV.

[18]This allows for the zero-point motion of the ions at 0 K. See, M. T. Yin and M. L. Cohen, Phys. Rev. B **29**, 6996 (1984); L. Brewer, Lawrence Berkeley Laboratory Report No. LBL-3720 (unpublished).

[19]O. Jepson and O. K. Andersen, Solid State Commun. **9**, 1763 (1971).

[20]A. Zunger, Phys. Rev. B **17**, 626 (1978).

[21]M. S. Hybertsen and S. G. Louie, Phys. Rev. Lett. **55**, 1418 (1985).

[22]K. J. Chang, S. Froyen, and M. L. Cohen, Solid State Commun. **50**, 105 (1984); S. Fahy, K. J. Chang, S. G. Louie, and M. L. Cohen (unpublished).

[23]This underestimates the gap in diamond by 20% compared with experiment, as we expect from local-density-functional theory.

[24]J. W. McClure, Carbon **7**, 425 (1967).

[25]This follows from the fact that minus the exchange-correlation energy density $-\varepsilon_{xc}(\mathbf{r})\rho(\mathbf{r})$ is an increasing convex function of $\rho(\mathbf{r})$ (see Ref. 14).

[26]L. M. Falicov, *Group Theory and its Physical Applications* (University of Chicago Press, 1966), pp. 133—138.